Available online at www.sciencedirect.com
SCIENCE DIRECT®
International Journal of Thermal Sciences 45 (2006) 829–840
International Journal of Thermal Sciences
www.elsevier.com/locate/ijts

Thermodynamic analysis and parametric study of an irreversible regenerative-intercooled-reheat Brayton cycle

S.K. Tyagi [a], G.M. Chen [a,*], Q. Wang [a], S.C. Kaushik [b]

[a] *Institute of Refrigeration and Cryogenics, Zhejiang University, Hangzhou 310027, People's Republic of China*
[b] *Centre for Energy Studies, Indian Institute of Technology, Delhi, New Delhi 110016, India*

Received 21 February 2005; received in revised form 18 October 2005; accepted 18 October 2005

Available online 30 January 2006

Abstract

An irreversible cycle model of a regenerative-intercooled-reheat Brayton heat engine along with a detailed parametric study is presented in this paper. The power output and the efficiency are optimized with respect to the cycle temperatures for a typical set of operating conditions. It is found that there are optimal values of the turbine outlet temperature, intercooling, reheat and cycle pressure ratios at which the cycle attains the maximum power output and efficiency. But the optimal values of these parameters corresponding to the maximum power output are different from those corresponding to the maximum efficiency for the same set of operating condition. The maxima of the power output and efficiency again changes as any of the cycle parameters is changed. The maximum power point and the maximum efficiency point exist but the power output corresponding to the maximum efficiency is found to be lower than that can be attained. The optimum operating parameters, such as the turbine outlet temperature, intercooling, reheat and cycle pressure ratios etc. corresponding to the maximum power output and corresponding to the maximum efficiency are obtained and discussed in detail. This cycle model is general and some of the results obtained by earlier workers can be derived directly from the present cycle model as a special case.

Keywords: Intercooled-reheat-Brayton heat engine cycle; Regenerator; Turbine; Compressor; Power output; Thermodynamic efficiency

1. Introduction

Thermodynamic efficiency is one of the important parameter among gas power cycles and has a major impact on the operating cost, especially due to the limited resources of fuel. In recent years concerted efforts have been made in different areas of gas turbine technologies with the main objective of improving the cycle efficiency [1–22]. In this pursuit, particularly for the last two decades, gas turbine industry has seen phenomenal achievements in different fields such as aerodynamics, material, blade cooling, fabrication technologies etc. With these advance technologies implemented, gas turbines have been developed with a high inlet turbine temperature (approaching to 1500 °C) and simple cycle efficiency 40 percent or above [1,2]. Another approach for improving cycle efficiency of the gas turbine is to modify the Brayton cycle.

There are several ways to modify a Brayton cycle, some of them have been reported in the literature [1–22] which have been studied in recent years include regeneration [4–11], isothermal heat addition [12–17], intercooled compression [18–20], reheat expansion [21] and their combination [1,2, 18–22] called as "complex Brayton cycle". The thermodynamics analysis of the above mentioned models exhibits that the efficiency of a Brayton cycle can be improved significantly provided an optimal value of intercooling and/or cycle pressure ratio is used [1,8,18–21].

Some work in this direction has been carried out on the evaluation of a complex Brayton cycle [1,2] using some standard software. As pointed out by Mathioudakis [3] that the main disadvantage of the methods based on the computational models is that although they provide information for a specific gas turbine, they do not give an idea about the generality of their predictions or about the factors governing the studied phenom-

* Corresponding author.
E-mail addresses: sudhirtyag@yahoo.com (S.K. Tyagi), gmchen@zju.edu.cn (G.M. Chen).

1290-0729/$ – see front matter
doi:10.1016/j.ijthermalsci.2005.10.011

Nomenclature

A	area ..... m^2
C	mass flow rate times specific heat ..... $kW\,K^{-1}$
N	number of transfer units
P^*	dimensionless power output
$(P^*)_{max}$	dimensionless maximum point of the power output
P^*_{max}	dimensionless maximum point of the optimized power output
P^*_m	dimensionless maximum power point at η_{max}
Q	heat transfer rates ..... kW
R_{pi}	intercooling pressure ratio
R_{ph}	reheat pressure ratio
R_p	cycle pressure ratio
S	isentropic/entropy ..... $kJ\,K^{-1}$
T	temperature ..... K
U	overall heat transfer coefficient .... $kW\,m^{-2}\,K^{-1}$
1, 2, 3, 4, 5, 6, 7, 8	state points

Greek letters

η	efficiency
$(\eta)_{max}$	maximum efficiency
η_{max}	maximum point of the optimized efficiency
η_m	optimum efficiency corresponding to P^*_{max}
ε	effectiveness
γ	specific heat ratio
α	$=(R_{pi}/R_{ph})^{1-1/\gamma}$

Subscripts

η	corresponding to the maximum point of thermodynamic efficiency
C	compressor/cold-side
H	heat source/hot-side
L	sink/cold-side
max	maximum
P^*	corresponding to the maximum point of power output
P^*_{max}	corresponding to the maximum point of the optimized power output
P^*_m	corresponding to the maximum point of power output at η_{max}
opt	optimum operating condition
R	regenerator
S	ideal/isentropic
T	turbine
W	working fluid
1	initial/entrance
2	final/outlet

enal. The analytical studies, when they can be performed of course, are best suited for deriving this type of information. In the present paper the effects of some important cycle parameters, such as the turbine outlet temperature, intercooling, reheat and cycle pressure ratios on the thermodynamic performance of this complex Brayton cycle is studied by a means of analytical relations [3–20] using the concept of finite time thermodynamics [23–25]. The analysis presented in this paper, demonstrates which are the main parameters governing changes in performance variables and provides simple relations among the different cycle parameters to estimate these changes. Thus, the use of analytical relations allows an understanding of the effects of different cycle parameters, such as the turbine outlet temperature, intercooling, reheat and cycle pressure ratios etc. and provides a means for a quick estimation of such effects in a wide range.

2. System description

The T–S diagram of an irreversible regenerative-intercooled-reheat Brayton cycle heat engine is shown on Fig. 1. As can be seen from Fig. 1, the working fluid enters the first compressor at state point 1 and is compressed up to state point 2 (ideally up to state point 2S) and then enters the first heat sink where it is cooled down up to state point 3 by rejecting the heat to the finite heat capacity heat sink whose temperature varies from T_{C1} to T_{C2}. The working fluid again enters the second compressor and is compressed up to state point 4 (ideally up to state point 4S) and then enters the regenerator where it is heated up to state point 4R by the exhaust of a low pressure

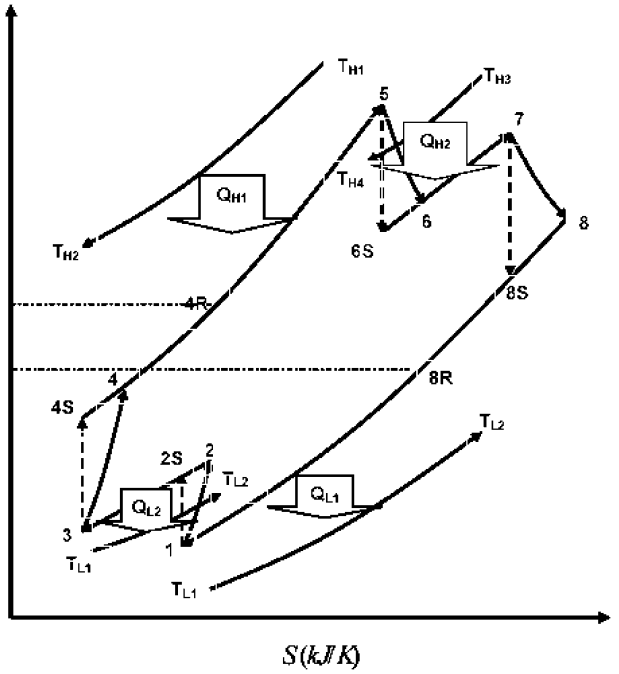

Fig. 1. T–S diagram of an intercooled-reheat-regenerative Brayton cycle.

turbine. The working fluid leaving the regenerator enters the first heat source and is heated up to state point 5 by the finite heat capacity heat source whose temperature varies from T_{H1} to T_{H2}. Then it enters the high pressure turbine and expands up to state point 6 (ideally up to state point 6S) and then enters the second heat source where it is heated up to state point 7

by the finite heat capacity heat source whose temperature varies from T_{H3} to T_{H4}. The working fluid again enters the low pressure turbine and expands up to state point 8 (ideally up to state point 8S) and enters the regenerator where it partly transfers its heat to the outlet of the second compressor and is cooled down up to state point 8R. Finally, the working fluid enters the second heat sink and is cooled down up to state point 1 by rejecting the heat to the finite heat capacity heat sink whose temperature varies from T_{L1} to T_{L2}, thereby, completing the cycle. Thus, we study the closed version 1-2-3-4-4R-5-6-7-8-8R-1 of an irreversible intercooled-regenerative-reheat Brayton cycle with the nonisentropic compression and expansion processes for the finite heat capacity of external reservoirs. The thermodynamic analysis of the cycle based on different laws is given in the end (see Appendix A).

3. Some characteristic curves

It is seen from Eqs. (A.13)–(A.14) that P and η are the functions of a single variable T_8, for a given set of operating conditions. Thus using Eqs. (A.13)–(A.14) and a typical set of operating parameters such as $R_{\rm pi} = 5$, $T_{H1} = T_{H3} = 1500$ K, $\varepsilon_{H1} = \varepsilon_{H2} = \varepsilon_{L1} = \varepsilon_{L2} = \varepsilon_R = \eta_{C1} = \eta_{C2} = \eta_{T1} = \eta_{T2} = 0.90$, $R_{\rm ph} = 8$, $C_{H1} = C_{H2} = C_{L1} = C_{L2} = 1.0$ kW K^{-1}, $T_{L1} = T_{C1} = 300$ K, and $C_W = 0.95$ kW K^{-1}, we have plotted some characteristic curves for the power output and the corresponding thermodynamic efficiency against the turbine outlet temperature (T_8) and between the power output and thermodynamic efficiency, and obtained the results as below.

3.1. Power output and thermodynamic efficiency vs T_8

The variations of the dimensionless power output and the corresponding thermodynamic efficiency against the outlet temperature of the low pressure turbine (T_8) are shown in Fig. 2(a)–(b) for a given set of operating parameters mentioned above. It is seen from these figures that the power output and the thermodynamic efficiency first increase and then decrease as T_8 is increased. Thus, there are optimal values of T_8 at which the power output and the corresponding thermodynamic efficiency attain their maximum values for a typical set of operating conditions. Also the optimal value of T_8 corresponding to the maximum power point is different and lower than that of the optimal value of T_8 corresponding to the maximum efficiency point, i.e. $(T_{8,\rm opt})_{P^*} < (T_{8,\rm opt})_\eta$ as can be seen from these figures. Again the optimal value of T_8 will change, if any of these operating parameters is changed. Thus, using Fig. 2(a)–(b) and a typical set of operating parameters mentioned above, we can give some optimal criteria for the optimal values of T_8 corresponding to the point of the maximum power output and the maximum efficiency as:

$$(T_{8,\rm opt})_{P^*} < T_{8,\rm opt} < (T_{8,\rm opt})_\eta \tag{1}$$

where $(T_{8,\rm opt})_{P^*}$ and $(T_{8,\rm opt})_\eta$ are respectively, the optimal values of T_8, corresponding the maximum point of power output and thermodynamic efficiency while $T_{8,\rm opt}$, is the optimum obtainable value of T_8 which exists somewhere between those two extreme points, mentioned above. Thus, Eq. (1) gives the optimal criterion for the outlet temperature of the low pressure

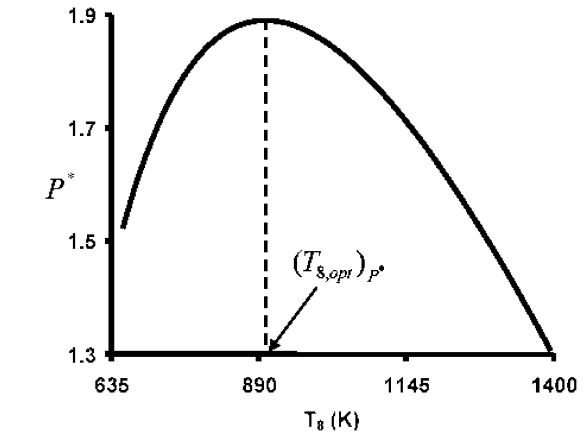

(a)

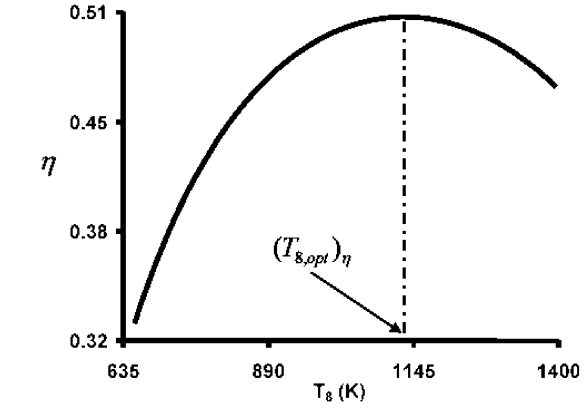

(b)

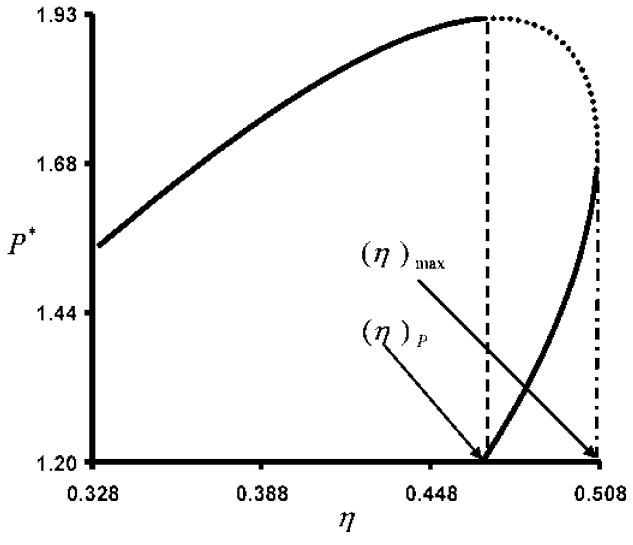

(c)

Fig. 2. The variations of (a) dimensionless power (b) thermodynamic efficiency with the turbine outlet temperature (T_8) and (c) dimensionless power vs thermodynamic efficiency, while the operating parameters are chosen as $T_{H1} = T_{H3} = 1500$ K, $R_{\rm pi} = 5$, $R_{\rm ph} = 8$, $\varepsilon_{H1} = \varepsilon_{H2} = \varepsilon_{L1} = \varepsilon_{L2} = \varepsilon_R = \eta_{C1} = \eta_{C2} = \eta_{T1} = \eta_{T2} = 0.90$, $C_{H1} = C_{H2} = C_{L1} = C_{L2} = 1.0$ kW K^{-1}, $T_{L1} = T_{C1} = 300$ K, and $C_W = 0.95$ kW K^{-1}.

turbine of an irreversible regenerative-intercooled-reheat Brayton cycle for a given set of operating parameters.

3.2. Power output vs thermodynamic efficiency

The variation of the dimensionless power output against the thermodynamic efficiency is shown in Fig. 2(c). It is seen from the Fig. 2(c) that the power output is not a monotonic function of the thermodynamic efficiency. The power output first increases and then decreases as the thermodynamic efficiency is increased. Thus, there is an optimal value of thermodynamic efficiency at which the power output attaints its maximum value for a typical set of operating parameters. Also the maximum power point and the maximum efficiency point exist but the power output at the point of the maximum efficiency is lower than that can be attained, as seen from Fig. 2(c). When the power output is situated in the region of the $(P^*)_{\max} \sim (\eta)_{\max}$ curve with a positive slope, it will decrease as the corresponding thermodynamic efficiency is decreased and vice-versa. Obviously, these regions are not optimal. It is thus clear that the maximum power output should be situated in the region of the $(P^*)_{\max} \sim (\eta)_{\max}$ curve with the negative slope. When the power output falls in this region, it will increase as the thermodynamic efficiency is decreased, and vice versa. Thus, it is shown that the optimal region of the thermodynamic efficiency should be determined by the relation:

$$(\eta)_{\max} \leqslant (\eta)_{\text{opt}} \leqslant (\eta)_{P^*} \tag{2}$$

where $(\eta)_{\max}$, $(\eta)_{\text{opt}}$ and $(\eta)_{P^*}$ are, respectively, the maximum point of the thermodynamic efficiency, the optimal obtainable efficiency and the efficiency corresponding to the maximum point of power output, as can be seen from Fig. 2(c).

The physical meaning of the above mentioned results can be explained in different ways, based on the irreversibility associated with the cycle, as well as on the concept of the energy saving. For example, if the temperature at state point 8 (T_8) is too low (lower than T_{L2}) then the regenerative effect is negative. In other words, the heat will be in the reverse direction i.e. from the outlet of the second compressor to the outlet of the low pressure turbine and hence, the utility of the regenerator will vanish. Also, if the temperature at state point 8 (T_8) is too high (higher than T_{H3}) then the heat will flow directly from the source to the sink, again, the utility of the reheat will vanish. Thus, between these two limits mentioned above, there are optimal values of T_8 at which the cycle attains its maximum performance for a given set of operating parameters. Again, if the low pressure turbine produces more work, then the power output of the cycle will be higher and the outlet temperature (T_8) will be lower, resulting a less energy transfer by the regenerator and hence, a lower value of the cycle efficiency. Also, if the low pressure turbine produces less work, then the power output of the cycle will be lower and the outlet temperature (T_8) will be higher, resulting a more energy transfer by the regenerator and hence, a higher value of the cycle efficiency. As a result, we get the curves shown in Fig. 2(a)–(c).

So far we have given some optimal criteria based on the outlet temperature of the low pressure turbine, of an irreversible regenerative-intercooled-reheat Brayton cycle for a typical set of operating parameters. We will further give some other optimal criteria based of different cycle parameters such as intercooling, reheat and cycle pressure ratios, component efficiencies etc. as below.

4. Maximum performance parameters

Based on Fig. 2(a) and Eq. (1), we observed that there is optimal value of T_8 at which the cycle attains its maximum power output for a given set of cycle parameters. Thus, using Eq. (A.13) and its most extreme condition $\frac{\partial P}{\partial T_8} = 0$, we can prove that the optimal value of T_8 corresponding to the maximum point of the optimized power output, is determined by the following equation:

$$(T_{8,\text{opt}})_{P_{\max}} = \frac{-B_1 + \sqrt{B_1^2 - A_1 C_1}}{A_1} \tag{3}$$

where the different parameters are given as:

$$A_1 = a_{14} - a_{14}^2/a_{16}^2, \qquad B_1 = a_{15} - a_{14}a_{15}/a_{16}^2$$
$$C_1 = a_{17} - a_{15}^2/a_{16}^2$$
$$a_{14} = a_7^2 - 4Aa_9, \qquad a_{15} = a_7 a_8 - 2Aa_{10}$$
$$a_{16} = (a_7 a_{12} - 4Aa_{13})/a_{12} \quad \text{and} \quad a_{17} = a_8^2 - 4Aa_{11}$$

Substituting the value of $(T_{8,\text{opt}})_{P_{\max}}$ and a typical set of operating parameters into Eqs. (A.13), (A.14), (A.12) and (A.9a–j), we can calculate the maximum value of the optimized power output and corresponding thermodynamic efficiency, i.e. $P_{\max}$ and η_m, and the optimum operating temperatures of other state points, which are listed in Tables 1 and 2 for different values of intercooling and reheat pressure ratios. Using the intercooling and reheat pressure ratios:

$$(R_{p,\text{opt}})_{P_{\max}} = \frac{P_H}{P_L} = \frac{P_H}{P_2}\frac{P_2}{P_L} = (T_{4S}/T_3)^{k/(k-1)}(R_{\text{pi,opt}})_{P_{\max}} \tag{4}$$

$$(R_{p,\text{opt}})_{P_{\max}} = \frac{P_H}{P_L} = \frac{P_H}{P_6}\frac{P_6}{P_L} = (T_7/T_{8S})^{k/(k-1)}(R_{\text{ph,opt}})_{P_{\max}} \tag{5}$$

we can also calculate the cycle pressure ratio corresponding to the maximum value of the optimized power output $(R_{p,\text{opt}})_{P_{\max}}$, for different values of the intercooling and reheat pressure ratios, as listed in Tables 1 and 2.

Again we observed from Fig. 2(b) that there is optimal value of T_8 at which the cycle attains its maximum thermodynamic efficiency. Thus Eq. (A.14) and its extremal condition $\frac{\partial \eta}{\partial T_8} = 0$, we can further give the optimal value of T_8 corresponding to the maximum point of the optimized thermodynamic efficiency, as:

$$(T_{8,\text{opt}})_{\eta_{\max}} = \frac{-B_2 + \sqrt{B_2^2 - A_2 C_2}}{A_2} \tag{6}$$

where the parameters are given as below:

Table 1
Effects of R_{pi} on the maximum power output, the corresponding efficiency, state point temperatures and the cycle pressure ratio, for a given set of cycle parameters as mentioned in Fig. 2

R_{pi}	$T_{1,opt}$	$T_{2,opt}$	$T_{2S,opt}$	$T_{3,opt}$	$T_{4S,opt}$	$T_{4,opt}$	$T_{4R,opt}$	$T_{5,opt}$	$T_{6S,opt}$	$T_{6,opt}$	$T_{7,opt}$	$T_{8,opt}$	$T_{8S,opt}$	$T_{8R,opt}$	P^*_{max}	η_m	$R_{p,opt}$
1.0	363	363	363	309	662	701	1058	1437	744	813	1402	1097	1064	741	1.79	0.582	14.4
1.5	357	405	400	315	621	655	1019	1431	741	810	1401	1060	1022	696	1.91	0.601	16.2
2.5	349	465	454	324	574	602	975	1425	738	807	1401	1016	974	643	2.03	0.612	18.6
3.5	344	509	493	330	545	569	948	1421	736	805	1401	990	945	611	2.08	0.612	20.3
4.5	341	545	524	335	525	546	929	1418	735	803	1400	972	924	589	2.10	0.608	21.7
5.5	339	575	551	339	509	528	915	1416	734	802	1400	958	909	571	2.11	0.603	22.8
6.5	337	601	575	343	496	514	903	1415	733	801	1400	947	896	557	2.11	0.598	23.7
7.5	335	625	596	346	486	501	894	1413	732	800	1400	937	886	545	2.10	0.592	24.5
8.5	334	646	615	349	477	491	886	1412	731	800	1400	929	877	535	2.10	0.586	25.2
9.5	332	666	632	352	469	482	879	1411	731	799	1400	923	870	526	2.09	0.58	25.9
10.5	331	684	648	355	462	474	872	1410	730	798	1400	917	863	518	2.08	0.574	26.5
11.5	330	701	663	357	456	467	867	1410	730	798	1400	911	857	511	2.07	0.569	27.0
12.5	329	716	678	359	450	460	862	1409	730	798	1400	907	852	505	2.05	0.563	27.5
13.5	328	731	691	362	445	455	858	1408	729	797	1400	902	847	499	2.04	0.558	28.0
14.5	328	745	704	364	441	449	853	1408	729	797	1400	898	843	494	2.03	0.552	28.4
15.5	327	759	716	366	436	444	850	1407	729	797	1400	895	839	489	2.02	0.547	28.8
16.5	326	772	727	367	432	440	846	1407	729	796	1399	891	835	485	2.00	0.542	29.2
17.5	326	784	738	369	429	435	843	1406	728	796	1399	888	832	481	1.99	0.537	29.5
18.5	325	796	749	371	425	431	840	1406	728	796	1399	885	828	477	1.98	0.532	29.9
19.5	325	807	759	372	422	428	837	1405	728	796	1399	883	825	473	1.96	0.528	30.2

Table 2
Effects of R_{pi} on the maximum efficiency, the corresponding power output, state point temperatures and the cycle pressure ratio, for a given set of cycle parameters as mentioned in Fig. 2

R_{ph}	$T_{1,opt}$	$T_{2,opt}$	$T_{2S,opt}$	$T_{3,opt}$	$T_{4S,opt}$	$T_{4,opt}$	$T_{4R,opt}$	$T_{5,opt}$	$T_{6S,opt}$	$T_{6,opt}$	$T_{7,opt}$	$T_{8,opt}$	$T_{8S,opt}$	$T_{8R,opt}$	P^*_{max}	η_m	$R_{p,opt}$
1.0	316	522	501	332	374	379	700	1386	1386	1386	1484	736	653	414	1.65	0.664	7.6
1.5	320	527	507	332	396	403	733	1390	1238	1254	1465	770	693	439	1.85	0.671	9.2
2.5	325	535	514	334	425	435	778	1397	1075	1107	1444	816	746	473	2.02	0.665	11.7
3.5	328	541	520	334	445	458	810	1401	980	1022	1432	849	784	497	2.09	0.657	13.6
4.5	331	545	524	335	461	476	835	1405	914	963	1423	875	814	515	2.12	0.648	15.3
5.5	333	549	527	336	475	490	855	1408	865	919	1417	896	838	531	2.13	0.639	16.8
6.5	335	552	530	336	486	503	873	1410	826	885	1412	914	859	544	2.13	0.631	18.2
7.5	336	555	533	336	496	514	889	1413	794	856	1408	931	878	555	2.13	0.623	19.5
8.5	338	557	535	337	505	523	903	1415	768	832	1405	945	894	566	2.12	0.616	20.6
9.5	339	559	537	337	513	532	916	1417	745	812	1402	958	909	575	2.11	0.609	21.7
10.5	340	561	539	337	520	540	927	1418	724	794	1399	970	923	583	2.10	0.603	22.8
11.5	342	563	541	338	527	548	938	1420	707	778	1397	981	935	591	2.09	0.597	23.7
12.5	343	565	543	338	533	555	948	1421	691	764	1395	992	947	598	2.07	0.591	24.7
13.5	344	566	544	338	539	561	957	1422	676	751	1393	1001	958	605	2.06	0.585	25.6
14.5	345	568	546	338	544	567	966	1424	663	739	1391	1010	968	612	2.04	0.580	26.4
15.5	345	569	547	338	549	573	974	1425	651	729	1390	1019	978	618	2.03	0.575	27.3
16.5	346	571	548	339	554	578	982	1426	640	719	1388	1027	987	623	2.01	0.571	28.1
17.5	347	572	549	339	559	583	990	1427	630	710	1387	1035	996	629	2.00	0.565	28.8
18.5	348	573	551	339	563	588	997	1428	620	701	1386	1042	1004	634	1.99	0.561	29.6
19.5	348	574	552	339	568	593	1004	1429	612	693	1385	1049	1012	639	1.97	0.556	30.3

$$A_2 = a_{14} - b_{10}^2/b_{12}^2, \qquad B_2 = a_{15} - b_{10}b_{11}/b_{12}^2$$

$$C_2 = a_{17} - b_{11}^2/b_{12}^2$$

$$b_9 = b_7a_{13} - b_8a_{12}, \qquad b_{10} = b_9a_{15} - K_4a_{14}$$

$$b_{11} = (b_9a_{17} - K_4a_{15}) \quad \text{and} \quad b_{12} = K_4a_7 + 2AK_5 - b_8b_9$$

Substituting the value of $(T_{8,opt})_{\eta_{max}}$ and a typical set of operating parameters into Eqs. (A.14), (A.13), (A.12) and (A.9a–j), we can find the maximum value of the optimized thermodynamic efficiency and corresponding power output, i.e. η_{max} and P_m, and the optimum operating temperatures of other state points, which are also listed in Tables 3 and 4 for different values of intercooling and reheat pressure ratios, Again, using the intercooling and reheat pressure ratios

$$(R_{p,opt})_{\eta_{max}} = \frac{P_H}{P_L} = \frac{P_H}{P_2}\frac{P_2}{P_L} = (T_{4S}/T_3)^{k/(k-1)}(R_{pi,opt})_{\eta_{max}} \tag{7}$$

$$(R_{p,opt})_{\eta_{max}} = \frac{P_H}{P_L} = \frac{P_H}{P_6}\frac{P_6}{P_L} = (T_7/T_{8S})^{k/(k-1)}(R_{ph,opt})_{\eta_{max}} \tag{8}$$

we can further calculate the optimal value of cycle pressure ratio corresponding to the maximum point of the optimized

Table 3
Effects of R_{ph} on the maximum power output, the corresponding efficiency, state point temperatures and the cycle pressure ratio, for a given set of cycle parameters as mentioned in Fig. 2

R_{pi}	$T_{1,opt}$	$T_{2,opt}$	$T_{2S,opt}$	$T_{3,opt}$	$T_{4S,opt}$	$T_{4,opt}$	$T_{4R,opt}$	$T_{5,opt}$	$T_{6S,opt}$	$T_{6,opt}$	$T_{7,opt}$	$T_{8,opt}$	$T_{8S,opt}$	$T_{8R,opt}$	P_m^*	η_{max}	$R_{p,opt}$
1.0	362	362	362	309	629	664	1272	1467	760	831	1404	1339	1332	732	1.10	0.450	12.1
1.5	355	403	398	314	584	614	1242	1463	758	828	1404	1312	1302	684	1.21	0.476	13.1
2.5	347	463	451	322	538	562	1198	1457	755	825	1404	1268	1253	632	1.31	0.493	15.1
3.5	343	508	491	327	513	534	1165	1452	752	822	1403	1235	1217	604	1.36	0.495	16.9
4.5	341	544	524	332	497	515	1139	1448	750	820	1403	1209	1187	584	1.39	0.492	18.5
5.5	339	575	551	336	485	502	1118	1445	749	818	1403	1187	1163	570	1.41	0.488	19.9
6.5	337	602	575	339	476	491	1100	1443	747	817	1402	1168	1142	559	1.42	0.482	21.3
7.5	336	626	597	342	469	483	1085	1441	746	816	1402	1152	1124	550	1.42	0.476	22.6
8.5	335	648	617	345	463	476	1071	1439	745	815	1402	1137	1108	542	1.43	0.470	23.8
9.5	334	668	635	348	458	471	1059	1437	744	814	1402	1124	1093	536	1.42	0.464	24.9
10.5	333	687	652	350	454	466	1048	1435	743	813	1402	1113	1080	530	1.42	0.458	26.1
11.5	332	705	667	352	450	461	1038	1434	743	812	1402	1102	1069	525	1.42	0.452	27.1
12.5	332	721	682	355	447	457	1029	1433	742	811	1402	1092	1058	521	1.41	0.446	28.1
13.5	331	737	696	357	444	454	1020	1431	741	810	1401	1083	1048	517	1.40	0.441	29.1
14.5	330	752	709	358	442	451	1013	1430	741	810	1401	1075	1039	513	1.39	0.435	30.1
15.5	330	766	722	360	439	448	1005	1429	740	809	1401	1067	1030	510	1.39	0.430	31.0
16.5	330	779	734	362	437	445	999	1428	740	809	1401	1060	1022	507	1.38	0.425	31.9
17.5	329	792	746	364	435	443	992	1427	739	808	1401	1053	1015	504	1.37	0.420	32.8
18.5	329	804	757	365	433	441	986	1427	739	808	1401	1047	1008	501	1.36	0.415	33.6
19.5	328	816	767	367	432	439	981	1426	739	807	1401	1041	1001	499	1.35	0.410	34.4

Table 4
Effects of R_{ph} on the maximum efficiency, the corresponding power output, state point temperatures and the cycle pressure ratio, for a given set of cycle parameters as mentioned in Fig. 2

R_{ph}	$T_{1,opt}$	$T_{2,opt}$	$T_{2S,opt}$	$T_{3,opt}$	$T_{4S,opt}$	$T_{4,opt}$	$T_{4R,opt}$	$T_{5,opt}$	$T_{6S,opt}$	$T_{6,opt}$	$T_{7,opt}$	$T_{8,opt}$	$T_{8S,opt}$	$T_{8R,opt}$	P_m^*	η_{max}	$R_{p,opt}$
1.0	317	523	502	329	361	365	869	1410	1410	1410	1487	924	862	421	1.03	0.524	6.9
1.5	320	527	506	329	373	377	922	1417	1262	1278	1468	982	928	438	1.19	0.544	7.9
2.5	324	534	513	330	394	401	983	1426	1098	1130	1447	1047	1003	466	1.33	0.549	9.3
3.5	327	539	518	331	413	422	1020	1431	1001	1044	1435	1087	1048	488	1.38	0.543	10.8
4.5	330	543	522	332	429	439	1047	1435	934	984	1426	1115	1080	507	1.41	0.535	12.3
5.5	332	547	526	332	442	455	1068	1438	884	939	1420	1136	1105	523	1.42	0.526	13.6
6.5	334	550	529	333	455	468	1085	1441	844	904	1415	1154	1125	537	1.42	0.518	14.9
7.5	336	553	532	333	466	481	1100	1443	811	874	1411	1169	1142	550	1.42	0.510	16.2
8.5	337	556	534	333	476	492	1112	1445	784	850	1407	1181	1156	561	1.42	0.502	17.4
9.5	339	559	537	334	486	503	1123	1446	760	829	1404	1192	1169	572	1.41	0.494	18.6
10.5	340	561	539	334	495	513	1133	1448	739	810	1401	1202	1180	582	1.40	0.486	19.8
11.5	342	563	541	334	503	522	1142	1449	721	794	1399	1211	1190	591	1.39	0.479	20.9
12.5	343	565	543	335	511	531	1150	1450	705	779	1397	1219	1199	600	1.38	0.473	22.0
13.5	344	567	545	335	519	539	1157	1451	690	766	1395	1226	1207	608	1.37	0.466	23.1
14.5	345	569	547	335	526	547	1164	1452	676	754	1393	1233	1215	616	1.35	0.460	24.2
15.5	346	571	548	335	533	555	1171	1453	664	743	1392	1239	1222	623	1.34	0.454	25.2
16.5	347	572	550	336	539	562	1176	1454	653	733	1390	1245	1229	630	1.33	0.448	26.2
17.5	348	574	551	336	545	569	1182	1455	642	723	1389	1250	1235	637	1.32	0.442	27.3
18.5	349	575	553	336	551	575	1187	1455	632	715	1388	1255	1241	643	1.30	0.437	28.3
19.5	350	577	554	336	557	582	1192	1456	623	706	1387	1260	1246	650	1.29	0.431	29.3

thermodynamic efficiency $(R_{p,opt})_{\eta_{max}}$, for different values of the intercooling and reheat pressure ratios, as given in Tables 3 and 4.

Since the intercooling and reheat pressure ratios are among the important parameters of an intercooled-reheat Brayton cycle, we will continue to discuss the effects of these (intercooling and reheat) pressure ratios on the performance of an irreversible regenerative-intercooled-reheat Brayton cycle heat engine to further reveal the general characteristics of this cycle.

Using the above results and a set of operating parameters which are similar to those given in Tables 1–4, we have plotted some performance characteristic curves among different cycle parameters for both cases. That is, the maximum power output and the corresponding thermodynamic efficiency case, as well as the maximum thermodynamic efficiency and the corresponding power output case, at a given set of operating conditions, and the results are shown on Figs. 3–9.

4.1. Effects of intercooling and reheat pressure ratios

It is seen from Tables 1 and 3 that the outlet temperatures of the intercooling compressor and the inlet temperature of the second compressor as well as the cycle compression ratio increase while the temperatures of all other state points decrease

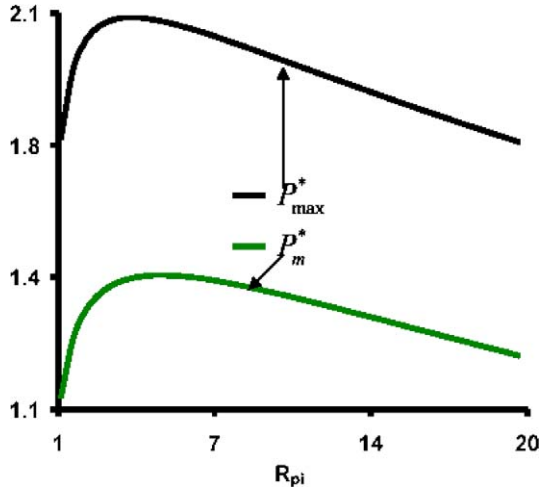

(a)

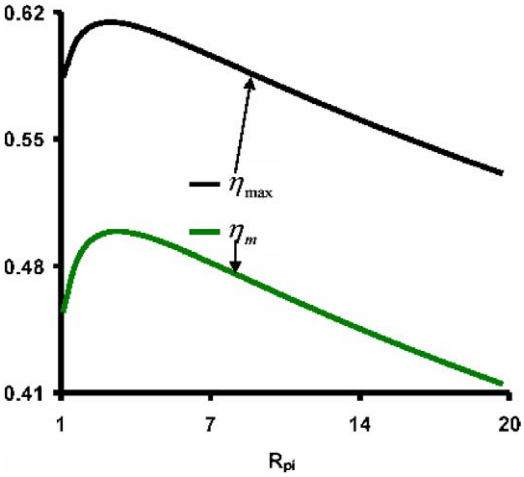

(b)

Fig. 3. The variations of (a) dimensionless optimized power (b) optimized thermodynamic efficiency with intercooling pressure ratio (R_{pi}), while the other cycle parameters are the same as in Fig. 2.

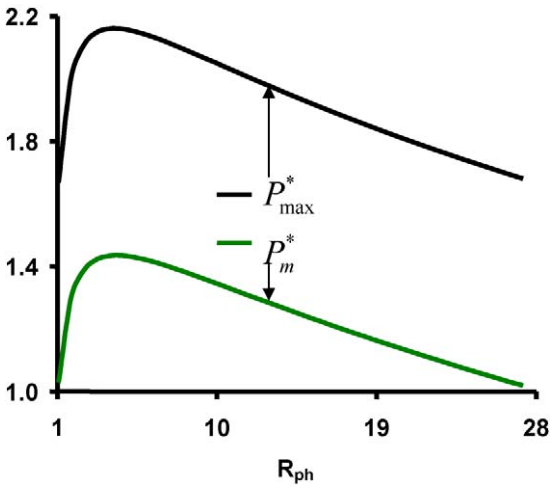

(a)

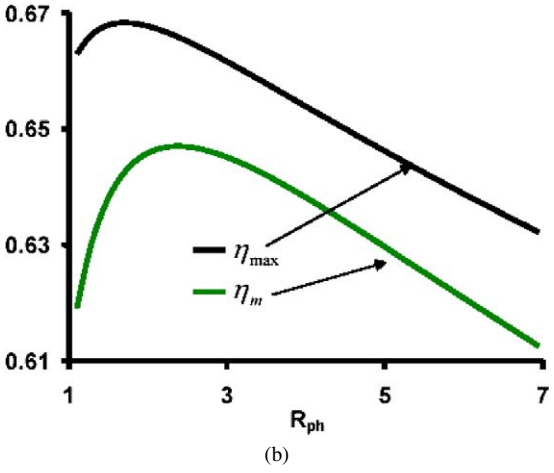

(b)

Fig. 4. The variations of (a) dimensionless optimized power (b) optimized thermodynamic efficiency with reheat pressure ratio (R_{ph}), while the other cycle parameters are the same as in Fig. 2.

as the intercooling pressure ratio increases. Whereas, the outlet temperatures of the high pressure turbine and the inlet temperature of the low pressure turbine decrease while the temperatures of all other state points as well as the cycle pressure ratio increase with increasing the reheat pressure ratio, as can be seen from Tables 2 and 4. On the other hand, the maximum power output and the corresponding thermodynamic efficiency as well as the maximum thermodynamic efficiency and the corresponding power output, first increase and then decrease as the either pressure ratio is increased [Figs. 3 and 4]. Thus it is seen clearly from these figures and Tables 1–4 that there are the optimal values of the intercooling and reheat pressure ratios at which the optimized power output and the corresponding thermodynamic efficiency, as well as the maximum thermodynamic efficiency and the corresponding power output attain their maximum values, i.e., $(P^*_{max})_{max}$, $(\eta_m)_{max}(\eta_{max})_{max}$ and $(P^*_m)_{max}$ for a given cycle parameters. But the maximum values of the optimized thermodynamic efficiency and the corresponding power output are lower than those of the maximum values of the optimized power output and the corresponding thermodynamic efficiency for the same of operating parameters, as can be seen from these Figs. 3 and 4 and Tables 1–4. Also, the optimum values of intercooling and reheat pressure ratios are different for different parameters. In other words, the optimum values of the intercooling and reheat pressure ratios at the maximum point of the optimized power output are different and higher than those of the optimum values of the intercooling and reheat pressure ratios at the maximum point of the optimized thermodynamic efficiency. This conclusion will provide some important theoretical instruction for the optimal design and operation of an irreversible regenerative-intercooled-reheat Brayton cycle heat engine.

In fact, the physical meaning of Figs. 3–5 and Tables 1–4 may be clearly explained from Fig. 1, in different ways. For example, if cycle pressure ratio tends to unity (as the intercooling and reheat pressure ratios are always less than the cycle pressure ratio), the heat will flow directly from the source to the sink, so no real cycle is performed. Again, if cycle pressure ratio tends to the reservoirs temperature ratio $(T_{H1}/T_{L1})^{\gamma/(\gamma-1)}$, the heat transfer rates to and from the cycle tends to zero, again no real cycle is performed. Thus at the above mentioned limits, the sig-

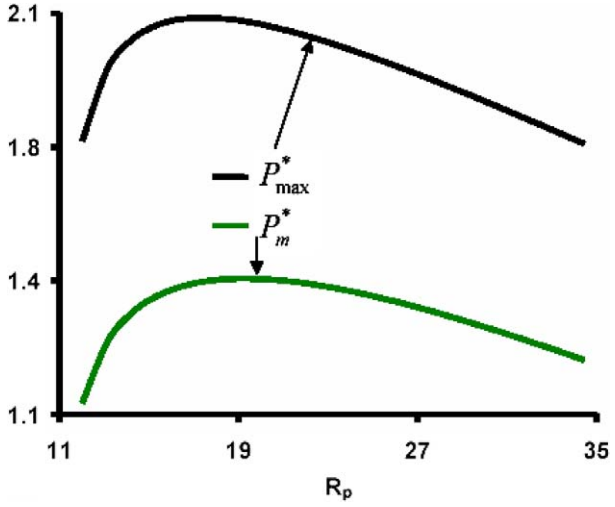

(a)

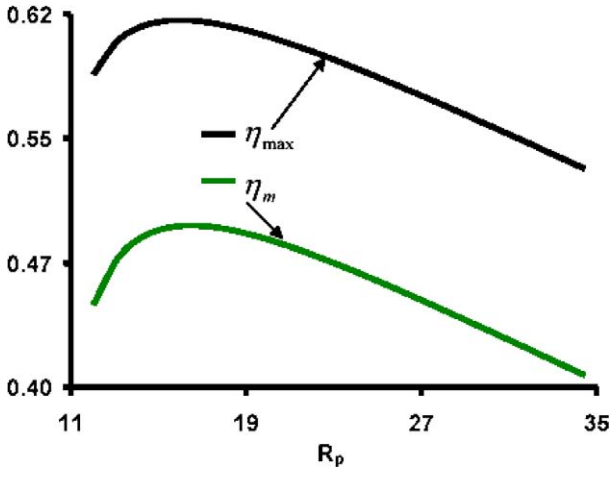

(b)

Fig. 5. The variations of (a) dimensionless optimized power (b) optimized thermodynamic efficiency with cycle pressure ratio (R_p), while the other cycle parameters are the same as in Fig. 2.

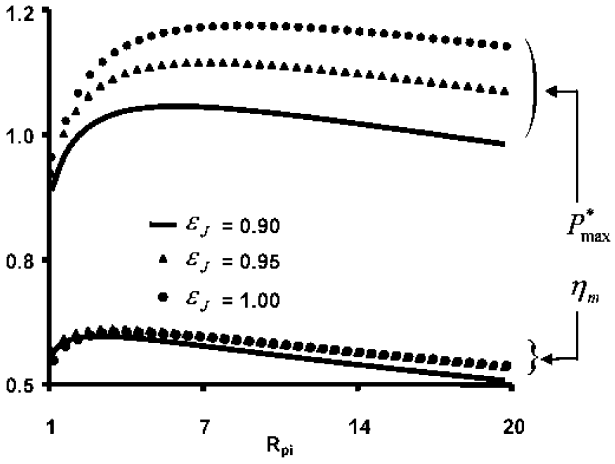

Fig. 6. The variations of dimensionless optimized power and the corresponding thermodynamic efficiency with R_{pi}, for different values of various effectiveness (ε's), while the other cycle parameters are the same as in Fig. 2.

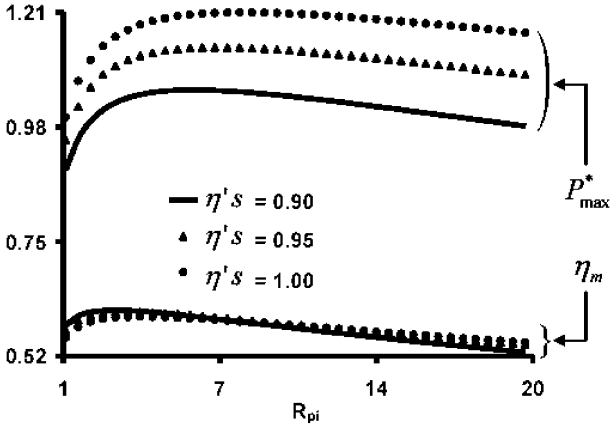

Fig. 7. The variations of dimensionless optimized power and the corresponding thermodynamic efficiency with R_{pi}, for different values of component efficiencies (η's), while the other cycle parameters are the same as in Fig. 2.

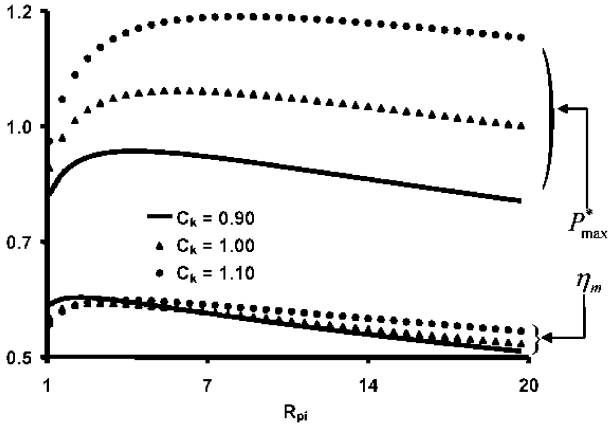

Fig. 8. The variations of dimensionless optimized power and the corresponding thermodynamic efficiency with R_{pi}, for different values of various heat capacitance rates in the external reservoirs (C_k's), while the other cycle parameters are the same as in Fig. 2.

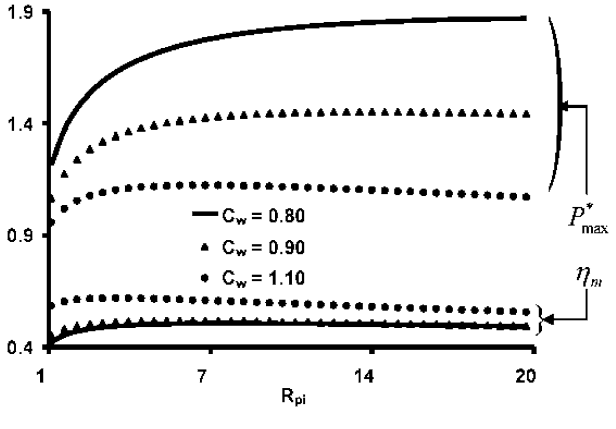

Fig. 9. The variations of dimensionless optimized power and the corresponding thermodynamic efficiency with R_{pi}, for different values of heat capacitance rate of the working fluid (C_W), while the other cycle parameters are the same as in Fig. 2.

nificant cycle cannot be formed, so the power output and corresponding thermodynamic efficiency tend to zero. Hence, there are necessarily some optimal values of the intercooling, reheat and cycle pressure ratios between unity and $(T_{H1}/T_{L1})^{\gamma/(\gamma-1)}$, at which the optimized power output and corresponding thermodynamic efficiency as well as the optimized thermodynamic efficiency and the corresponding power output attain their maximum values, i.e. $(P^*_{\max})_{\max}$, $(\eta_m)_{\max}(\eta_{\max})_{\max}$ and $(P^*_m)_{\max}$ for a typical set of operating parameters.

It is also important to note the fact that the intercooling and reheat pressure ratios are always more than unity and less than the cycle pressure ratio, i.e.:

$$1 < R_{\text{pi}} < R_p \tag{9}$$

$$1 < R_{\text{ph}} < R_p \tag{10}$$

When $R_{\text{pi}} = 1$ or $R_{\text{pi}} = R_p$ and $R_{\text{ph}} = 1$ or $R_{\text{ph}} = R_p$, the cycle becomes an irreversible simple Brayton cycle, which has been discussed by a number of workers [4–11]. Similarly, when $R_{\text{ph}} = 1$ or $R_{\text{ph}} = R_p$, the cycle becomes an irreversible intercooled Brayton cycle without reheater which also has been discussed by other workers [18–20], and if $R_{\text{pi}} = 1$ or $R_{\text{pi}} = R_p$ the cycle becomes an irreversible reheat Brayton cycle [21]. Obviously, the optimal values of the intercooling and reheat pressure ratios are different for different operating states. It is important how to choose the optimal values of these pressure ratios in the investigation of an irreversible regenerative-intercooled-reheat Brayton cycle heat engine. Hence, according to Tables 1–4 and/or Figs. 3 and 4 we can, in principle, determine the rational range of the optimal values of the intercooling and reheat pressure ratios, as:

$$(R_{\text{pi,opt}})_{P^*_{\max}} > R_{\text{pi,opt}} > (R_{\text{pi,opt}})_{\eta_{\max}} \tag{11}$$

$$(R_{\text{ph,opt}})_{P^*_{\max}} > R_{\text{ph,opt}} > (R_{\text{ph,opt}})_{\eta_{\max}} \tag{12}$$

where $(R_{\text{pi,opt}})_{P^*_{\max}}$, $(R_{\text{pi,opt}})_{\eta_{\max}}$ and $(R_{\text{ph,opt}})_{P^*_{\max}}$, $(R_{\text{ph,opt}})_{\eta_{\max}}$ are, respectively, the intercooling and reheat pressure ratios at the maximum points of the optimized power output and thermodynamic efficiency, while $R_{\text{pi,opt}}$ and $R_{\text{ph,opt}}$ are, the optimal obtainable values of the intercooling and reheat pressure ratios, respectively. Using Eqs. (11)–(12) and Fig. 5(a) and (b), we can give another optimum criterion for the cycle pressure ratio, as:

$$(R_{p,\text{opt}})_{P^*_{\max}} > R_{p,\text{opt}} > (R_{p,\text{opt}})_{\eta_{\max}} \tag{13}$$

where $(R_{p,\text{opt}})_{P^*_{\max}}$ and $(R_{p,\text{opt}})_{\eta_{\max}}$ are, respectively, the optimal values of the cycle pressure ratios at the maximum points of the optimized power and thermodynamic efficiency, while $R_{p,\text{opt}}$, is the optimal obtainable value of the cycle pressure ratio. According to Eqs. (11)–(13) and Tables 1–4, we can also give the optimum criteria for the temperatures of the various state points. The criteria will be helpful for engineers to optimally design and operate an irreversible regenerative-intercooled-reheat Brayton cycle heat engine.

4.2. Effects of effectiveness

The variations of the dimensionless maximum power output and the corresponding thermodynamic efficiency with respect to the intercooling pressure ratio for the different values of effectiveness (ε_{H1}, ε_{H2}, ε_{L1}, ε_{L2} and ε_R) for a typical set of operating parameters are shown in Fig. 6. It is seen from Fig. 6 that there is an optimal value of the intercooling pressure ratio at which the cycle attains its maximum power output and thermodynamic efficiency, for a given set of operating parameters. But the optimal value of the intercooling pressure ratio corresponding to the maximum point of the optimized power output is different and more than that of the optimal value of the intercooling pressure ratio corresponding to the maximum point of the optimized efficiency. In other words, $(R_{\text{pi,opt}})_{P^*_{\max}} > (R_{\text{pi,opt}})_{\eta_{\max}}$ for the same set of operating parameters. Again, the maximum power output and the corresponding thermodynamic efficiency, further enhance as the effectiveness of these heat exchangers are increased. Also the increment in both parameters is small for lower values of R_{pi} while it is reverse in the case of higher values of R_{pi}, which can be explained in terms of external and internal irreversibilities associated with the cycle.

4.3. Effects of components efficiencies

Fig. 7 show the variations of the dimensionless maximum power output and the corresponding thermodynamic efficiency with respect to the intercooling pressure ratio at different values of components efficiencies (η_{C1}, η_{C2}, η_{T1} and η_{T2}) and for a typical set of other operating parameters. It is seen from Fig. 7 that there are optimal values of the intercooling pressure ratio at which the cycle attains its maximum power output and thermodynamic efficiency, for a given set of operating parameters. Again, the maximum power output further enhances as the efficiency of these components are increased, but it is reverse in the case of thermodynamic efficiency for lower values of R_{pi}. In other words, the thermodynamic efficiency goes down as the components efficiencies are increased for lower values of R_{pi} but it is reverse in the case of higher values of R_{pi}. The increment in power output is less for lower values of R_{pi} while it is reverse in the case of higher values of R_{pi}, for the same set of operating parameters. On the other hand, the increment in thermodynamic efficiency is more for the lower and higher values of R_{pi}, while it is reverse for the intermediate range.

The results obtained in Figs. 6 and 7 can be explained in terms of external and internal irreversibilities. For example, the higher are the effectiveness of these heat exchangers, the lesser will be the irreversibility associated with the cycle and hence, the higher will be performance of the cycle, as can be seen from Fig. 6. Again, as the efficiencies of different components are increased, the outlet temperatures of these components go down and hence, the internal irreversibility associated with the cycle is decreased, resulting, the higher power output of the cycle. Also, as mentioned in the earlier section that the turbine outlet temperature decreases with increasing the turbine efficiency and hence, the regenerative heat transfer rate decreases, resulting, the lower cycle efficiency in the region of lower values of R_{pi}. But for higher values of intercooling pressure ratio, the turbine and compressor efficiencies are more effective because of two main reasons. First, in the region of higher values of intercooling pressure ratio, the power consumption in the com-

pressors increase significantly and the effect of the regenerator decreases, second, the power output of turbines increase significantly by increasing the cycle (up to the certain values of R_{pi} and R_{ph}) pressure ratio, as a result, a better overall performance of the cycle for the higher component efficiencies. Since, for higher values of intercooling pressure ratio, the power consumption in the compressor is much higher but decreases significantly with increasing the compressor efficiency, as a result, the overall cycle efficiency increases, in the region of higher values of intercooling pressure ratio, as can be seen from Fig. 7.

4.4. Effects of heat capacitance rates

The dimensionless maximum power output and the corresponding thermodynamic efficiency against the intercooling pressure ratio are plotted in Figs. 8 and 9 for the different values of various heat capacitance rates (C_{H1}, C_{H2}, C_{L1}, C_{L2} and C_W) at a given set of cycle parameters. It is seen from these figures that the maximum power output and the corresponding thermodynamic efficiency first increase and then decrease as the intercooling pressure ratio increases. It is also found that the maximum power output further enhances as the heat capacitance rates of the external reservoirs (C_{H1}, C_{H2}, C_{L1}, and C_{L2}) are increased, while it is reverse in the case of the working fluid heat capacitance rate. On the other hand, the thermodynamic efficiency first goes down in the region of lower values of R_{pi} which is reverse in the region of higher values of R_{pi}, for the heat capacitance rates of the external reservoirs. While the thermodynamic efficiency always enhances as the heat capacitance rate of the working fluid is increased. The increment in power output is less for lower values of R_{pi} and more for higher values of R_{pi} for all heat capacitance rates (C_{H1}, C_{H1}, C_{L1}, C_{L2} and C_W), while it is reverse in the case of the thermodynamic efficiency, for the working fluid heat capacitance rate. Whereas, the increment in thermodynamic efficiency is more for the lower and higher values of R_{pi}, for the heat capacitance rates of the external reservoirs (C_{H1}, C_{H2}, C_{L1}, and C_{L2}).

The results obtained in Figs. 8 and 9 can be explained in terms of irreversibility associated with the cycle. For example, the higher are the heat capacitance rates of the external fluids, the lesser will be the temperature difference between the cycle and the external reservoirs and hence, lesser will be irreversibility associated with the cycle, resulting, the better performance of the cycle, as can be seen from Fig. 8. Similarly, the higher is heat capacitance rate the of the working fluid, lesser will be irreversibility associated with the cycle, but higher will be the power consumption in the compressors due to the increase in the mass flow rate of the working fluid within the cycle, resulting, the higher efficiency but lower net power output of the cycle, as can be seen from Fig. 9.

We have given some optimal criteria based on different cycle parameters of an irreversible regenerative-intercooled-reheat Brayton cycle for a typical set of operating parameters. It is also important to note that the present cycle model is general and the results obtained by earlier workers [3–11,18–22] are the special cases of this cycle model. For example, if $R_{pi} = R_{ph} = 1.0$, and $\eta_C = \eta_T < 1.0$, are chosen, the results obtained in this paper are identical to those obtained in Refs. [3–11] and if $R_{ph} = 1.0$ and $\eta_C = \eta_T < 1.0$, are chosen, the results are identical to those obtained in Refs. [18–21], $C_H = C_L \to \infty$ and $\eta_C = \eta_T = 1.0$, are chosen, the results obtained in this paper are identical to those obtained in Ref. [22].

5. Conclusions

An irreversible cycle model of a regenerative-intercooled-reheat Brayton heat engine along with a detailed parametric study is presented in this paper. The power output and the thermodynamic efficiency are optimized with respect to the cycle temperatures for a typical set of operating conditions. The maximum power output is found to be an increasing function of the effectiveness of different heat exchangers, heat capacitance rates in the external reservoirs, component efficiencies while it is found to be a decreasing function of the working fluid heat capacitance rate. On the other hand, there are optimal values of the intercooling, reheat and cycle pressure ratios and the turbine outlet temperature at which the cycle attains the maximum power output and maximum thermodynamic efficiency. Also, the optimal values of these parameters corresponding to the maximum power output are found to be different generally higher from those corresponding to the maximum efficiency. The maxima of the power output and efficiency again changes as any of the cycle parameters is changed. The maximum power point and the maximum efficiency point are obtained but the power output corresponding to the maximum efficiency is found to be lower than that can be attained. The optimum operating region for different cycle parameters, such as the turbine outlet temperatures, the intercooling, reheat and cycle pressure ratios etc. corresponding to the maximum power output and the maximum thermodynamic efficiency are obtained and discussed in detail. Hence, the results obtained in this cycle model will be useful to understand and to improve the design and performance of a Brayton cycle with some new designs and modifications in order to achieve the growing demand of power with the environmental protection using the advance technology.

Acknowledgement

Sincere thanks are due to DunAn Artificial Environmental Equipment Co., Ltd. Zhejiang, China, for the financial assistance through a collaborative research project with Zhejiang University, Hangzhou 310027, People's Republic of China.

Appendix A. Thermodynamic analysis

According to the cycle model shown in Fig. 1, the various heat transfer rates to and from the cycle can be written as in appendix [7–20].

$$\begin{aligned} Q_{H1} &= (UA)_{H1}(LMTD)_{H1} = C_W(T_5 - T_{4R}) \\ &= C_{H1}(T_{H1} - T_{H2}) = C_{H1,\min}\varepsilon_{H1}(T_{H1} - T_{4R}) \qquad \text{(A.1)} \\ Q_{H2} &= (UA)_{H2}(LMTD)_{H2} = C_W(T_7 - T_6) \end{aligned}$$

$$= C_{H2}(T_{H3} - T_{H4}) = C_{H2,\min}\varepsilon_{H2}(T_{H3} - T_6) \quad (A.2)$$

$$Q_{L1} = (UA)_{L1}(LMTD)_{L1} = C_W(T_{8R} - T_1)$$

$$= C_{L1}(T_{L2} - T_{L1}) = C_{L1,\min}\varepsilon_{L1}(T_{8R} - T_{L1}) \quad (A.3)$$

$$Q_{L2} = (UA)_{L2}(LMTD)_{L2} = C_W(T_2 - T_3)$$

$$= C_{L2}(T_{C2} - T_{C1}) = C_{L2,\min}\varepsilon_{L2}(T_2 - T_{C1}) \quad (A.4)$$

$$Q_R = (UA)_R(LMTD)_R = C_W(T_8 - T_{8R})$$

$$= C_W(T_{4R} - T_4) = C_W\varepsilon_R(T_8 - T_4) \quad (A.5)$$

where $(UA)_J$'s ($J = H1, H2, L1, L2, R$) are, the overall heat transfer coefficient–area products while ε_J's, are respectively, the effectiveness on the source-, reheat-, sink-, intercooler- and the regenerative-side heat exchangers, defined as [6–8,10–20]:

$$\varepsilon_k = \frac{\{1 - e^{-N_k(1-C_{km})}\}}{\{1 - C_{km}e^{-N_k(1-C_{km})}\}} \quad (C_{km} = C_{k,\min}/C_{k,\max}) \quad \text{and}$$

$$\varepsilon_R = \frac{N_R}{1 + N_R} \quad (A.6)$$

where and C_k's and C_W, are, respectively, the heat capacitance rates (mass flow rate multiplied by the specific heat) of the external reservoirs and within the cycle. $C_{k,\min} = \min(C_k, C_W)$, $C_{k,\max} = \max(C_k, C_W)$, (here $k = H1, H2, L1, L2$) and N_J's $\{= (UA)_J/C_W\}$, are, the number of transfer units, based on the minimum thermal capacitance, while $(LMTD)_J$'s, are, the Log Mean Temperature Differences on their respective side heat exchangers, defined as [4–8,10–20]:

$$(LMTD)_{H1} = \big[(T_{H2} - T_4) - (T_{H1} - T_5)\big] \times \left(\ln\frac{(T_{H2} - T_4)}{(T_{H1} - T_5)}\right)^{-1} \quad (A.7a)$$

$$(LMTD)_{H2} = \big[(T_{H4} - T_6) - (T_{H3} - T_7)\big] \times \left(\ln\frac{(T_{H4} - T_6)}{(T_{H3} - T_7)}\right)^{-1} \quad (A.7b)$$

$$(LMTD)_{L1} = \big[(T_{8R} - T_{L2}) - (T_1 - T_{L1})\big] \times \left(\ln\frac{(T_{8R} - T_{L2})}{(T_1 - T_{L1})}\right)^{-1} \quad (A.7c)$$

$$(LMTD)_{L2} = \big[(T_2 - T_{C2}) - (T_3 - T_{C1})\big] \times \left(\ln\frac{(T_2 - T_{C2})}{(T_3 - T_{C1})}\right)^{-1} \quad (A.7d)$$

$$(LMTD)_R = \big[(T_8 - T_{4R}) - (T_{8R} - T_4)\big] \times \left(\ln\frac{(T_8 - T_{4R})}{(T_{8R} - T_4)}\right)^{-1} \quad (A.7e)$$

With the help of Fig. 1, the efficiencies of the compressors and turbines can be written as [3–20]:

$$\eta_{C1} = \frac{(T_{2S} - T_1)}{(T_2 - T_1)}, \qquad \eta_{C2} = \frac{(T_{4S} - T_3)}{(T_4 - T_3)}$$

$$\eta_{T1} = \frac{(T_5 - T_6)}{(T_5 - T_{6S})} \quad \text{and} \quad \eta_{T2} = \frac{(T_7 - T_8)}{(T_7 - T_{8S})} \leqslant 1.0 \quad (A.8)$$

Now, from Eqs. (A.1)–(A.5) and (A.8), we have [11–20]:

$$T_{8R} = (1 - \varepsilon_R)T_8 + \varepsilon_R T_4 \quad (A.9a)$$

$$T_{4R} = (1 - \varepsilon_R)T_4 + \varepsilon_R T_8 \quad (A.9b)$$

$$T_5 = (1 - x_1)T_{4R} + x_1 T_{H1} \quad (A.9c)$$

$$T_7 = (1 - x_2)T_6 + x_2 T_{H3} \quad (A.9d)$$

$$T_1 = (1 - y_1)T_{8R} + y_1 T_{L1} \quad (A.9e)$$

$$T_3 = (1 - y_2)T_2 + y_2 T_{C1} \quad (A.9f)$$

$$T_{2S} = (1 - \eta_{C1})T_1 + \eta_{C1}T_2 \quad (A.9g)$$

$$T_{4S} = (1 - \eta_{C2})T_3 + \eta_{C2}T_4 \quad (A.9h)$$

$$T_{6S} = \big(1 - \eta_{T1}^{-1}\big)T_5 + \eta_{T1}^{-1}T_6 \quad (A.9i)$$

$$T_{8S} = \big(1 - \eta_{T2}^{-1}\big)T_7 + \eta_{T2}^{-1}T_8 \quad (A.9j)$$

where $x_i = C_{H,\min}\varepsilon_H/C_w$ and $y_i = C_{L,\min}\varepsilon_L/C_w$ ($i = 1, 2$, $H = H1, H2$ and $L = L1, L2$). Rearranging Eqs. (A.9a–j), yields:

$$T_1 = a_1T_4 + b_1T_8 + c_1 \quad \text{and} \quad T_2 = aT_1 \quad (A.10a)$$

$$T_3 = a_2T_4 + b_2T_8 + c_2 \quad (A.10b)$$

$$T_{4S} = a_3T_4 + b_3T_8 + c_3 \quad (A.10c)$$

$$T_5 = a_4T_4 + b_4T_8 + c_4 \quad \text{and} \quad T_6 = bT_5 \quad (A.10d)$$

$$T_7 = a_5T_4 + b_5T_8 + c_5 \quad (A.10e)$$

$$T_{8S} = a_6T_4 + b_6T_8 + c_6 \quad (A.10f)$$

where the different parameters are below:

$$a_1 = (1 - \varepsilon_R)(1 - y_1), \qquad b_1 = \varepsilon_R(1 - y_1), \qquad c_1 = y_1T_{L1},$$

$$a_2 = a(1 - y_2)b_1, \qquad b_2 = a(1 - y_2)a_1$$

$$c_2 = \big\{a(1 - y_2)y_1 + y_1\big\}T_{L1}$$

$$a_3 = \eta_{C2} + (1 - \eta_{C2})a_2, \qquad b_3 = (1 - \eta_{C2})b_2$$

$$c_3 = (1 - \eta_{C2})c_2$$

$$a_4 = (1 - \varepsilon_R)(1 - x_1), \qquad b_4 = \varepsilon_R(1 - x_1)$$

$$c_4 = x_1T_{H1}$$

$$a_5 = b(1 - x_2)b_4, \qquad b_5 = b(1 - x_2)a_4$$

$$c_5 = b(1 - x_2)c_4 + x_2T_{H3}$$

$$a_6 = \big(1 - \eta_{T2}^{-1}\big)a_5, \qquad b_6 = \eta_{T2}^{-1} + \big(1 - \eta_{T2}^{-1}\big)b_5$$

$$c_6 = (1 - \eta_{T2}^{-1})c_5$$

$$a = \big(R_{\text{pi}}^{1-1/\gamma} + \eta_{C1} - 1\big)\eta_{C1}^{-1} \quad \text{and}$$

$$b = \big(1/R_{ph}^{1-1/\gamma} + \eta_{T1}^{-1} - 1\big)\eta_{T1}$$

Using the second law of thermodynamics in this case of a closed cycle 1-2*S*-3-4*S*-5-6*S*-7-8*S*-1 intercooled-reheat Brayton heat engine [18–20], we have:

$$T_{2S}T_{4S}T_{6S}T_{8S} = T_1T_3T_5T_7 \quad (A.11)$$

Substituting the values of intercooling and reheat pressure ratios i.e. $R_{\text{pi}}^{1-1/\gamma} = T_{2S}/T_1$, $R_{\text{ph}}^{1-1/\gamma} = T_{6S}/T_5$ and different temperatures from Eqs. (A.10a–f) into Eq. (A.11), we get a quadratic equation in T_4 and T_8, which on solving for T_4, yields [6,10,15,17,20]:

$$T_4 = \frac{-B + \sqrt{B^2 - 4AC}}{2A} \quad (A.12)$$

where the different parameters are below:

$$A = a_2a_5 - \alpha a_3a_6, \qquad B = a_7T_8 + a_8$$
$$C = a_9T_8^2 + a_{10}T_8 + a_{11}, \qquad \alpha = (R_{\rm pi}/R_{\rm ph})^{1-1/\gamma}$$
$$a_7 = a_2b_5 + a_5b_2 - \alpha(a_3b_6 + a_6b_3)$$
$$a_8 = a_2c_5 + a_5c_2 - \alpha(a_3c_6 + a_6c_3)$$
$$a_9 = b_2b_5 - \alpha b_3b_6$$
$$a_{10} = b_2c_5 + b_5c_2 - \alpha(b_3c_6 + b_6c_3) \quad \text{and}$$
$$a_{11} = c_2c_5 - \alpha c_3c_6$$

Using the first law of thermodynamics, the power output and the corresponding thermodynamic efficiency in this case of an irreversible regenerative-intercooled-reheat Brayton cycle heat engine, are given by [4–20]:

$$P = Q_{H1} + Q_{H2} - Q_{L1} - Q_{L2} = K_1 - \frac{a_{12}}{2A}\Big(-(a_7T_6 + a_8) + \sqrt{(a_7T_6 + a_8)^2 - 4A\big(a_9T_6^2 + a_{10}T_6 + a_{11}\big)}\Big) - a_{13}T_8 \tag{A.13}$$

$$\eta = \frac{P}{Q_{H1} + Q_{H2}} = \left[K_1 - \frac{a_{12}}{2A}\Big(-(a_7T_8 + a_8) + \sqrt{(a_7T_8 + a_8)^2 - 4A\big(a_9T_8^2 + a_{10}T_8 + a_{11}\big)}\Big) - a_{13}T_8\right] \times \left[K_2 - \frac{b_7}{2A}\Big(-(a_7T_6 + a_8) + \sqrt{(a_7T_6 + a_8)^2 - 4A\big(a_9T_6^2 + a_{10}T_6 + a_{11}\big)}\Big) - b_8T_8\right]^{-1} \tag{A.14}$$

where the different parameters are given as below:

$$K_1 = C_W\big\{(1 - ax_2)x_1T_{H1} + x_2T_{H3} + (1 - by_2)y_1T_{L1} + y_2T_{C1}\big\}$$
$$K_2 = C_W\{x_1T_{H1} + x_2T_{H3} + x_2c_4\}$$
$$K_3 = a_{12}K_3 - b_7K_2, \qquad K_4 = b_8K_2 - a_{13}K_3,$$
$$a_{12} = C_W\big\{x_1(1 - \varepsilon_R) + bx_2(1 - x_1)(1 - \varepsilon_R) + y_1\varepsilon_R + ay_2\varepsilon_R(1 - y_1)\big\}$$
$$b_8 = C_W\{x_1\varepsilon_R + bx_2b_4\}$$
$$b_7 = C_W\big\{x_1(1 - \varepsilon_R) + bx_2a_4\big\} \quad \text{and}$$
$$a_{13} = C_W\big\{x_1\varepsilon_R + bx_2(1 - x_1)\varepsilon_R + y_1(1 - \varepsilon_R) + ay_2(1 - \varepsilon_R)(1 - y_1)\big\}$$

References

[1] R. Bhargava, A. Peretto, A unique approach for thermoeconomic optimization of an intercooled, reheat, and recuperated gas turbine for cogeneration applications, J. Engrg. Gas Turbine Power 124 (2002) 881–891.

[2] I.G. Rice, Thermodynamic evaluation for gas turbine cogeneration cycle Part—II, Complex cycle analysis, J. Engrg. Gas Turbine Power 109 (1987) 8–15.

[3] K. Mathioudakis, Analysis of the effects of water injection on the performance of a gas turbine, J. Engrg. Gas Turbine Power 109 (1987) 489–495.

[4] C. Wu, R.S. Kiang, Power performance of a nonisentropic Brayton cycle, J. Engrg. Gas Turbines Power 113 (1991) 501–504.

[5] H.S. Leff, Thermal efficiency at maximum power output: New results for old engines, Amer. J. Phys. 55 (1987) 602–610.

[6] C.Y. Cheng, C.K. Chen, Power optimization of an endoreversible regenerative Brayton cycle, Energy 21 (1996) 241–247.

[7] O.M. Ibrahim, S.A. Klein, J.W. Mitchell, Optimum heat power cycles for specified boundary conditions, J. Engrg. Gas Turbines Power 113 (1991) 514–521.

[8] L. Chen, F. Sun, C. Wu, R.L. Kiang, Theoretical analysis of the performance of a regenerative closed cycle Brayton engine with internal irreversibilities, Energy Convers. Mgmt. 38 (1997) 871–877.

[9] V. Redcenco, J.V.C. Vargas, A. Bejan, Thermodynamic analysis of a gas turbine power plant with pressure drop irreversibilities, J. Energy Res. Tech. 129 (1998) 233–240.

[10] S.C. Kaushik, S.K. Tyagi, Finite time thermodynamic analysis of a nonisentropic regenerative Brayton heat engine, Int. J. Solar Energy 22 (2002) 141–151.

[11] A. Medina, J.M.M. Rocco, C. Hernandez, Regenerative gas turbine at maximum power density conditions, J. Phys. D: Appl. Phys. 29 (1996) 2802–2805.

[12] J. Vecchirelli, J.G. Kawall, J.S. Wallace, Analysis of a concept for increasing the efficiency of a Brayton cycle via isothermal heat addition, Int. J. Energy Res. 21 (1997) 113–127.

[13] S. Göktun, H. Yavuz, Thermal efficiency of a regenerative Brayton cycle with isothermal heat addition, Energy Convers. Mgmt. 40 (1999) 1259–1266.

[14] S.C. Kaushik, N. Singh, S.K. Tyagi, Thermodynamic evaluation of a modified steam regenerative Brayton heat engine for solar thermal power generation, J. Solar Energy Soc. India 9 (1999) 63–75.

[15] S.K. Tyagi, Finite time thermodynamic analysis and second law evaluation of thermal energy conversion systems, PhD thesis, CCS University, Meerut, India, June, 2000.

[16] L.B. Erbay, S. Göktun, H. Yavuz, Optimal design of the regenerative gas turbine engine with isothermal heat addition, Appl. Energy 68 (2001) 249–269.

[17] S.C. Kaushik, S.K. Tyagi, M.K. Singhal, Parametric study of an irreversible regenerative Brayton heat engine with isothermal heat addition, Energy Convers. Mgmt. 44 (2003) 2013–2025.

[18] C.Y. Cheng, C.K. Chen, Maximum power of an endoreversible intercooled Brayton cycle, Int. J. Energy Res. 24 (2000) 485–494.

[19] W. Wang, L. Chen, F. Sun, C. Wu, Performance analysis of an irreversible variable temperature heat reservoir closed intercooled regenerated Brayton cycle, Energy Convers. Mgmt. 44 (2003) 2713–2732.

[20] S.K. Tyagi, J. Chen, G. Lin, S.C. Kaushik, Effects of the intercooling on the performance of an irreversible regenerative Brayton heat engine cycle, Int. J. Ambient Energy (Communicated, 2004), submitted for publication.

[21] M.G. Negri di, M. Gambini, A. Peretto, Reheat and regenerative gas turbine for feed water repowering of steam power plant, in: ASME Turbo Expo., Houston, June 5–8, 1995.

[22] S.C. Kaushik, A. Chandra, H.S. Chandra, First and second-law analysis of an intercooled-reheat-regenerative gas turbine thermal power plant, Exergy – Int. J. 2 (3) (2005) 260–273.

[23] F.L. Curzon, B. Alhborn, Efficiency of Carnot heat engine at maximum power output, Amer. J. Phys. 43 (1975) 22–24.

[24] C. Wu, R.L. Kiang, Finite time thermodynamic analysis of a finite time Carnot heat engine with internal irreversibility, Energy 17 (1992) 1173–1178.

[25] A. Bejan, Theory of heat transfer irreversible power plants, Int. J. Heat Mass Transfer 31 (1988) 1211–1219.